PROBING ANOMALOUS TRIPLE BOSON VERTICES AT FUTURE e^+e^- COLLIDERS

Pat Kalyniak and Paul Madsen

Ottawa-Carleton Institute for Physics, Physics Department, Carleton University

1125 Colonel By Drive, Ottawa, Canada K1S 5B6

Nita Sinha and Rahul Sinha

Institute of Mathematical Sciences, CIT Campus Taramani,

Madras, India, 600113

Abstract

We explore the detection potential of the four lepton production processes $e^+e^- \to l^+\nu l'^-\overline{\nu}$ for anomalous contributions to the triple boson vertices at proposed future high energy colliders with center-of-mass energies of 500 GeV and 1 TeV. The predicted bounds are of the order of a few percent for the CP-even couplings κ_V (V=γ,Z) at the higher energy; we show that these limits can be improved by as much as a factor of two through suitable phase space cuts. A polarized beam facility, with its ability to access helicity information, could provide constraints on the vertices significantly tighter than those achievable from an analysis of total cross-section alone. The bounds on the CP-odd coupling $\tilde{\lambda}_V$ approach the indirect bounds from neutron electric dipole measurements while those on $\tilde{\kappa}_V$ are much looser. The asymmetries in experimental observables produced by such an explicitly CP violating triple vertex contribution are seen to be below the expected level of statistical precision of approximately 1.5%; asymmetries in the individual contributing

helicity amplitudes might however be detectable.

PACS number(s): 13.10.+q, 14.80.Er

I. INTRODUCTION

It will be possible to directly measure the Triple Boson Vertices (TBV) at future high energy e^+e^- colliders like the CERN Large Electron Positron Collider II (LEPII) [1,2] and the Next Linear Collider (NLC) [3–5]. These gauge boson self-couplings are a key prediction of the non-abelian $SU(2)_L \times U(1)_Y$ electroweak theory and, as yet, are only loosely constrained by indirect loop contributions and measurements of the $p\overline{p} \to W^{\pm}\gamma, W^{\pm}Z$, and W^+W^- processes. Both the D0 and CDF collaborations have now looked for $W\gamma$ [6,7], WZ [8], and W^+W^- [8,9] production in the data from the 1A run (1992-93). Present 95 % CL experimental limits are $-2.3 < \Delta\kappa_\gamma < 2.2$ (CDF) and $-1.6 < \Delta\kappa_\gamma < 1.8$ (D0) from $p\overline{p} \to W\gamma$ and $-1.0 < \Delta\kappa_V < 1.1$ (CDF) and $-2.6 < \Delta\kappa_V < 2.8$ (D0) from $p\overline{p} \to WW, WZ$. Two analyses of recent CLEO data [10] on the process b$\to s\gamma$ determine consistent limits of $-1.44 < \Delta\kappa_\gamma < 1.5$ [11] and $-0.41 < \Delta\kappa_\gamma < 1.22$ [12]. While these experimental bounds are compatible with the Standard Model (SM), they are still too weak to be considered a precision test of the theory.

The couplings of the W to the neutral gauge bosons γ and Z can be described in general by an effective Lagrangian with seven parameters. A standard parametrization of the vertices is [13]

$$\begin{aligned} L_{VWW}/g_V = {} & ig_1^V(W^\dagger_{\mu\nu}W^\mu V^\nu - W^\dagger_\mu V_\nu W^{\mu\nu}) + i\kappa_V W^\dagger_\mu W_\nu V^{\mu\nu} \\ & + \frac{i\lambda_V}{M_W^2} W^\dagger_{\lambda\mu} W^\mu_\nu V^{\nu\lambda} - f_4^V W^\dagger_\mu W_\nu(\partial^\mu V^\nu + \partial^\nu V^\mu) \\ & + f_5^V \epsilon^{\mu\nu\rho\sigma}(W^\dagger_\mu \overleftrightarrow{\partial}_\rho W_\nu)V_\sigma + i\tilde{\kappa}_V W^\dagger_\mu W_\nu \tilde{V}^{\mu\nu} \\ & + \frac{i\tilde{\lambda}_V}{m_W^2} W^\dagger_{\lambda\mu} W^\mu_\nu \tilde{V}^{\nu\lambda} \end{aligned}$$

where V represents either the photon or Z field and the overall couplings are $g_\gamma = e$ and $g_Z = e\cot\theta_W$.

Of the seven coupling parameters, $g_1^V, \kappa_V, \lambda_V$, and f_5^V parametrize CP respecting effective Lagrangian terms; their tree-level standard model values are

$$g_1^V = \quad \kappa_V = 1, \quad \lambda_V = f_5^V = 0$$

Most previous work on anomalous TBV contributions has concentrated on these CP-even couplings [13–15]. For a recent review see [16]. Predicted detection bounds on these couplings at the Large Hadron Collider (LHC) and an NLC with e^+e^- center of mass energy of 500 GeV or greater are at the percent level and better when a variety of processes is considered. This degree of sensitivity should be sufficient to measure the TBV at the level of Standard Model loop corrections [17] and certain extensions to the SM [18].

The couplings $f_4^V, \tilde{\kappa}_V$, and $\tilde{\lambda}_V$ parametrize vertex contributions that violate CP invariance. Since CP violation was first discovered in the neutral $K^o - \overline{K}^o$ system, a satisfactory explanation of its origin has been lacking. Within the $SU(2)_L \times U(1)_Y$ framework of the SM, CP violation occurs via the Kobayashi-Maskawa phase in the CKM matrix. Since the CKM matrix lies in the quark sector, a CP violating contribution to a leptonic process will appear to first order at the two-loop level in the SM; these CP-odd couplings are therefore zero at tree and one-loop level. One-loop effects are however possible in extensions to the SM; they manifest themselves in non-zero $f_4^V, \tilde{\kappa}_V$, and $\tilde{\lambda}_V$ of the order of 10^{-2} or smaller due to the loop suppression [19,18]. Such an explicitly CP violating contribution to the WWγ vertex is strongly constrained by neutron electric dipole measurements to be less than $\sim (10^{-4})$ [20]; the SU(2) symmetry then implies that a WWZ contribution should be similar in magnitude. Nevertheless, because these experimental constraints on a CP violating contribution to the TBV are indirect, they are no substitute for a direct search.

We have previously considered the purely leptonic processes

$$e^+e^- \rightarrow l^+\nu l^{-\prime}\overline{\nu} \tag{1}$$

with all possible charged lepton combinations in the final state as candidates for measuring the triple boson vertex. The details of that examination are given in [15]. Detection limits for the CP-even couplings κ_V, achievable through measurement of the total cross-section at energies of 500 GeV and 1 TeV were there determined. At $\sqrt{s} = 500$ GeV, we found

$$-2.5\%(\mu\tau) < \Delta\kappa_\gamma < +8.0\%(ee)$$

$$-4.5\%(\mu e) < \Delta\kappa_Z < +8.0\%(\mu e)$$

and at $\sqrt{s} = 1$ TeV,

$$-1.0\%(\mu\tau) < \Delta\kappa_\gamma < +3.5\%(\mu\tau, \mu e)$$
$$-1.5\%(\mu\tau) < \Delta\kappa_Z < +2.5\%(\mu\tau)$$

where the parentheses indicate which of the charged lepton combinations provide these tightest bounds.

In this paper, we extend our consideration of the processes of Eq.(1). The paper consists of two parts. In the first, we discuss means by which the above limits on the CP-even couplings κ_V might be improved. We discuss in Section II A the advantages offered by accessing the helicity information through a polarized beam facility and present in Section II B the improved limits achievable through the restriction of certain angular variables' phase space. In the second part of the paper, we examine the potential for detection of non-standard values for the CP-odd couplings $\tilde{\kappa}_V$ and $\tilde{\lambda}_V$. We present in Section III A our results for detection limits on the couplings $\tilde{\kappa}_V$ and $\tilde{\lambda}_V$, derived from both total and differential cross-section analyses. In Section III B we consider the possibility of asymmetries in certain CP odd variables as providing more sensitive indicators of CP violation than does the cross-section. We summarize in Section IV.

II. IMPROVING LIMITS FOR CP-EVEN COUPLINGS κ_V

A. Polarized Beams

In the energy ranges of LEP and higher, in contrast with the left-right symmetric physics of the QED dominated lower energies, helicity effects are expected to be important. These polarization effects might prove useful in the measurement of the triple boson vertices WWγ and WWZ. The possibility of using polarized e^+e^- beams to access the helicity information in a measurement of the TBV has been examined previously [1,21–23]. At LEPII energies, polarized beams are not expected to provide a substantial gain in sensitivity, but might help

to disentangle different anomalous contributions [1,21]. At higher energies, significantly improved limits on the couplings could be achieved with initial beam polarization [22,23].

Individual helicity amplitudes for a given process can differ in their dependence, both in form and magnitude, on the triple boson vertices. The contributions of different helicity amplitudes to the total cross-section can therefore provide constraints on κ_γ and κ_Z that are complementary to those obtained from the total cross-section. For instance, the $\mu^+\tau^-$ channel has contributions from only the $(+-+-)$ and $(-++-)$ helicity amplitudes. Our convention is to list the helicities of the four charged fermions as (e^+, e^-, l^+, l'^-). The $(+-+-)$ amplitude involves the neutrino exchange diagram of W-pair production, the $(-++-)$ amplitude does not. This diagram dominates the $(+-+-)$ amplitude as well as the total cross-section but unfortunately does not contain the trilinear couplings. The neutrino exchange diagram can therefore be thought of as a κ_V-independent "background" to the contributions of the triple boson vertex containing diagrams. The $(-++-)$ amplitude, and resulting cross-section, is free of the large κ_V-independent contribution of this diagram, and has therefore a relatively greater sensitivity to deviations $\Delta\kappa_V$. Without the dominant t-channel neutrino contribution however, the cross-section σ_{-++-} is much smaller than that of σ_{+-+-} ($\sigma_{-++-} \sim 10^{-2}\sigma_{+-+-}$), with consequently poorer statistical sensitivity. It therefore requires analysis to determine whether the improved sensitivity to $\Delta\kappa_V$ of σ_{-++-} will be sufficient to counter the loss of statistics, and ultimately provide more stringent limits.

To illustrate the scale of the possible improvements in the detection limits for the deviations $\Delta\kappa_V$, we examine the individual helicity amplitude contributions to the total cross-section for the $\mu^+\tau^-$ channel at $\sqrt{s} = 500$ GeV. The $\mu^+\tau^-$ channel is chosen because, with only two helicity amplitudes contributing, it provides the simplest demonstration of the principle. The other final state configurations present complications due to the larger number of contributing helicity amplitudes. Without the ability to measure the polarization of the final state fermions, what would actually be measured are the four different possible combinations of initial polarizations, $++, +-, -+$, and $--$, some of which would be sums over separate helicity amplitudes.

As before, we explore the sensitivity of the cross-sections to variations in κ_γ and κ_Z, but now also determine the percentage contribution of each helicity state to the total cross-section. We convert these percentages into effective component cross-sections, from which helicity detection limits on κ_γ and κ_Z can be determined. For reference, the Standard Model total cross-section for the $\mu^+\tau^-$ process at $\sqrt{s} = 500$ GeV, including also the charge conjugate channel $\mu^-\tau^+$, is σ_{SM}=0.0684 pb. The individual helicity state contributions to this total are determined to be, $\sigma_{SM}^{(+-+-)}$=0.0676 pb and $\sigma_{SM}^{(-++-)}$=0.0008 pb.

We show the results of the analysis in Fig. 1. The concentric solid lines are the $\pm 2\sigma$ contours for the $(+-+-)$ helicity state; the "disk" they define is very similar to that of the total cross-section. The four parallel diagonal dotted lines are the $\pm 2\sigma$ contours corresponding to the $(-++-)$ amplitude. This distinctive form is a consequence of the cancellations that occur between the photon and Z contributions to the $(-++-)$ amplitude for equal pairings of κ_γ and κ_Z. The SM Feynman rules for the couplings of γ and Z to massive leptons, plus the different coupling strengths of the two triple boson vertices γWW and ZWW, ensure that the κ-dependence of the $(-++-)$ amplitude can be schematically written as

$$M_{(-++-)} = \left(\frac{\kappa_\gamma - 1}{s} - \frac{\kappa_Z - 1}{s - M_Z^2} \right) (A) + (B) \tag{2}$$

Thus, for equal values of non-standard κ_γ and κ_Z and $s \gg M_Z^2$, the different contributions of the photon and Z bosons will nearly cancel.

Neither the $(+-+-)$ disk region or the $(-++-)$ bands independently offer significantly tighter constraints on κ_γ and κ_Z than did the unpolarized cross-section; the intersection of the former with the latter does however severely restrict the allowed domain. What had been a relatively large set of κ_γ, κ_Z pairings statistically indistinguishable from the Standard Model prediction is reduced to a significantly smaller union of two separate regions. Polarization measurements could therefore, in the specific case of the $\mu^+\tau^-$ final state, provide significantly tighter constraints on κ_γ and κ_Z than would the unpolarized cross-section. For instance, if we vary the couplings individually, keeping the other at its SM

value, we determine limits

$$0.99 < \kappa_Z < 1.01$$

$$0.99 < \kappa_\gamma < 1.01 \quad \text{and} \quad 1.08 < \kappa_\gamma < 1.09$$

which are a significant improvement on the bounds achievable from the unpolarized analysis.

For large center-of-mass energies, the cancellation between the photon and Z terms when $\kappa_\gamma = \kappa_Z$ results in a $(-++-)$ helicity amplitude contribution of less than about 1% of the total cross-section. When $\kappa_\gamma \neq \kappa_Z$ however, this amplitude can contribute a much larger portion of the total, the above cancellation being destroyed. A small percentage contribution of $(-++-)$ to the total cross-section is therefore characteristic of equal values for κ_γ and κ_Z and thus provides a characteristic "signature" of such pairings. More than merely helping to distinguish between the cases of equal or unequal κ_γ and κ_Z, the relative contribution of the $(-++-)$ amplitude could potentially serve as a characteristic "fingerprint" of a particular region of the κ_γ, κ_Z grid. A measurement of a non-standard cross-section can, in general, be attributed to any of an infinite set of pairings of κ_γ and κ_Z, these points lying on a contour of constant cross-section. Although indistinguishable by a simple measurement of total cross-section, these pairings will, in general, have very different characteristic helicity contributions. Thus, once a cross-section measurement had indicated a non-standard κ_γ, κ_Z pairing, the relative contributions of the helicity amplitudes to the total cross-section could differentiate between the sets of possible pairings responsible.

Similar analyses were performed for the other final state lepton pairings. The bounds from the other helicity amplitudes that contribute to these more complicated processes were generally seen to be too loose to provide any further constraint on the couplings.

B. Sensitivity Enhancing Cuts

In this Section, we examine the results of making various phase space cuts. We show in Fig. 2 the distributions for the angular variable $\cos\theta_{\tau^-}$ (where θ_{τ^-} is the angle between the

outgoing lepton and the incoming positron) for the $e^+e^- \to \mu^+\nu\tau^-\overline{\nu}$ process at $\sqrt{s} = 500$ GeV. The solid line corresponds to the Standard Model values, the dashed line to $\kappa_\gamma = \kappa_Z = 0.9$, and the dotted line to $\kappa_\gamma = \kappa_Z = 1.1$.

The strong peak in the distribution at $\cos\theta_{\tau^-} \simeq -1$ is a consequence of the t-channel neutrino exchange diagram of W pair production. This behaviour is repeated for the three other processes with different final state lepton configurations, but is less marked. There, the many extra diagrams beyond W pair production dilute the effect of the t-channel neutrino diagram.

For non-standard pairings of κ_γ and κ_Z, these angular distributions are generally somewhat enhanced in the regions of phase space away from this peak. Since the t-channel neutrino exchange diagram does not contain the triple boson vertex, the peak is relatively insensitive to the vertex couplings. This localization of the κ sensitivity to the "non-peak" regions of the θ_{l^-} phase space suggests the potential for maximizing the κ sensitivity by cutting on these variables to exclude the large non-sensitive peak contributions, and isolate the κ dependent plateau regions. Because, by making such a cut, we lose a significant portion of our total cross-section, we must distinguish between improving the *physical* sensitivity, as a percentage deviation from the SM total cross-section, and the *experimental* sensitivity, defined as the potential for detection of anomalous couplings.

The angular variables are not unique in their localization of sensitivity to κ_V. Another potential observable is $M_{l^+l'^-}$, the invariant mass of the outgoing charged lepton-antilepton pair. The sensitivity to non-standard κ_V is located predominantly in the middle region of the $M_{\mu\tau}$ distribution for the $\mu^+\tau^-$ process at $\sqrt{s} = 500$ GeV. A cut such as 30 GeV $< M_{\mu\tau} <$ 430 GeV would exclude the κ-insensitive contributions from the extreme low and high invariant mass regions of phase space. We can therefore consider making combined cuts, both an angular and invariant mass cut, in hopes of improving sensitivity.

To simplify matters, we restrict our study to the case $\kappa_\gamma = \kappa_Z$. Any limits derived with the angular cuts in place, although more constraining than those obtained by making no assumptions about the relationship between κ_γ and κ_Z, will still demonstrate the scale of

the improvements in sensitivity possible.

In Table I, for the $\mu\tau$ channel at $\sqrt{s} = 500$ GeV, we show the 2σ limits achievable for different combinations of angular and invariant mass cuts. Experimental beam-pipe detection limitations motivated our "weak" angular cut of $\theta_C = 0.95$; this cut itself removes a significant portion of the peak region of phase space. A "strong" cut θ_C was chosen so as to minimize the contribution of the non-sensitive peak, whilst maximizing the total cross-section. The choices of $\theta_C = 0.7$ and $\theta_C = 0.9$ were taken as representing the extremes of optimizing the two opposing requirements, $\theta_C = 0.9$ maximizes statistics and $\theta_C = 0.7$ excludes essentially all of the peak contribution.

We see that making a cut on the variables can significantly improve the limits for $\Delta\kappa < 0$, but has little effect for $\Delta\kappa > 0$. Also, the most restrictive combined cut of $\theta_C = 0.7$ and $100 < M_{\mu\tau} < 350$, despite a sizable decrease in cross-section, gives the tightest constraint on $\Delta\kappa < 0$ (but not for $\Delta\kappa > 0$). It seems that the improvement in physical sensitivity more than compensates for the loss of statistics.

The other channels, μ^+e^-, $\mu^+\mu^-$, and e^+e^-, because of the extra complexity due to the additional diagrams, do not as cleanly provide the possibility of sensitivity enhancing cuts. The additional κ_V dependent diagrams can contribute to the very regions of phase space that we previously considered excluding; a cut to exclude these regions of phase space can therefore be counter productive, with consequently no significant improvement in achievable coupling limits.

The bounds quoted in Table I are for a center of mass energy of 500 GeV. The sensitivity to κ is generally more evenly distributed over the available phase space at the higher energy of 1 TeV. Although the effect of the neutrino propagator is enhanced at higher energies, the contribution of this diagram becomes less significant as $\sqrt{s} \gg 2M_W$. There is therefore less motivation for excluding these angular regions to improve the limits on the κ couplings.

III. DETECTION POTENTIAL FOR CP-ODD COUPLINGS

We now extend our investigation to consider CP-odd couplings. The CP violating form factors $f_4, \tilde{\kappa}$, and $\tilde{\lambda}$ can, depending on the model and the kinematics, have both real and imaginary parts. The effects of the two different possibilities can be separated by examining the consequences of the CPT theorem and the unitarity condition. The CPT theorem postulates the invariance

$$< f|M|i >=< CPT(i)|M|CPT(f) > \tag{3}$$

where $|CPT(j) >$ represents the state $|j >$ transformed by CPT. It is very difficult to directly check this symmetry because it requires the interchange of initial and final states. It is more convenient to define a pseudo time reversal transformation, $\tilde{T}$, that transforms the kinematic observables of the initial and final state, as does T, but does not interchange the initial and final states.

In the Born approximation, unitarity of the S-matrix implies that the transition matrix, M, is hermitian. Thus, in the Born approximation M satisfies

$$M_{if} = M^*_{fi}$$

And so, with a hermitian transition matrix, the CPT theorem reduces to

$$< f|M|i >=< CP\tilde{T}(f)|M|CP\tilde{T}(i) >^* \tag{4}$$

The CPT theorem therefore provides a check on the hermiticity of the transition matrix M. Non-hermiticity of M, which is due to contributions beyond Born in which intermediate states can be on-shell, will manifest itself in violations of $CP\tilde{T}$.

We approximate our full four lepton production processes by W pair production for the purpose of discussion. If we define $A_{\lambda,\overline{\lambda}}$ as the tree level SM contribution to the transition matrix (with basis (-,0,+), the helicities of the W's) and $\delta A_{\lambda,\overline{\lambda}}$ as the deviation due to the CP violating couplings, $\delta A_{\lambda,\overline{\lambda}}$ can be compactly expressed as [24]

$$\delta A_{\lambda,\overline{\lambda}} = \begin{bmatrix} -i(\beta^{-1}\tilde{\kappa} + 4\gamma^2\beta\tilde{\lambda}) & -i\gamma(f_4 + \beta^{-1}\tilde{\kappa}) & 0 \\ -i\gamma(-f_4 + \beta^{-1}\tilde{\kappa}) & 0 & i\gamma(f_4 + \beta^{-1}\tilde{\kappa}) \\ 0 & i\gamma(-f_4 + \beta^{-1}\tilde{\kappa}) & i(\beta^{-1}\tilde{\kappa} + 4\gamma^2\beta\tilde{\lambda}) \end{bmatrix} \tag{5}$$

The coefficients in the above are $\gamma = \sqrt{s}/2m_W$ and $\beta^2 = 1 - \gamma^{-2}$.

Under the $CP\tilde{T}$ transformation, we must have

$$\delta A_{\lambda,\overline{\lambda}} \overset{CP\tilde{T}}{\rightarrow} \delta A^*_{-\overline{\lambda},-\lambda}$$

which requires $f_4, \tilde{\kappa}$, and $\tilde{\lambda}$ to be real. An imaginary component of the coupling parameters will break the $CP\tilde{T}$ symmetry, and so parametrizes the non-hermiticity of the transition matrix, the hallmark of beyond Born final state interactions. Such effects are small in a weakly coupled theory such as the SM, and so in what follows we concentrate on the case where all form factors are real.

Of the three CP-odd couplings, $\tilde{\kappa}$ and $\tilde{\lambda}$ are C-even and P-odd, f_4 is P-even and C-odd. Thus a non-zero f_4^γ is forbidden by electromagnetic gauge invariance. With $f_4^\gamma = 0$, the existence of a non-zero f_4^Z would imply that the W boson interactions intrinsically violate the SU(2) weak-isospin symmetry. There is, however, good empirical evidence for the validity of this symmetry. Accordingly, we assume also that $f_4^\gamma = f_4^Z = 0$ and restrict ourselves to the couplings $\tilde{\kappa}_\gamma, \tilde{\kappa}_Z, \tilde{\lambda}_\gamma$, and $\tilde{\lambda}_Z$ in the following Sections. Also, in the analysis of these CP-odd couplings, we restrict the CP-even couplings to their SM values, $\kappa_V = 1$ and $\lambda_V = 0$.

A. Detection Limits on $\tilde{\kappa}_V$ and $\tilde{\lambda}_V$

1. Total Cross-Section Measurements

We determine detection limits on $\tilde{\kappa}_V$ and $\tilde{\lambda}_V$ at two center-of-mass energies, 500 GeV and 1 TeV. For each of the four different types of four lepton channels, at each of the two energies, we fit parabolas to the dependence of the total cross-section on each of the couplings $\tilde{\kappa}_\gamma, \tilde{\kappa}_Z, \tilde{\lambda}_\gamma$, and $\tilde{\lambda}_Z$. The Standard Model cross-section σ_{SM}, multiplied by our

assumed integrated luminosity of 50 fb^{-1}, determines the expected number of events N, about which we assume a normal distribution. The detection limits, representing the magnitude of anomalous coupling required to give a 2σ deviation in the number of events, are listed below in Tables II and III.

The constraints on $\tilde{\kappa}_V$ from Table II are quite loose compared to the predicted bounds on the CP-even κ_V. The limits on κ_V approach the few percent level at the higher energy of $\sqrt{s} = 1$ TeV. The difference in sensitivity between the CP-even and CP-odd couplings can be attributed in part to the relative phase between the CP-odd and SM contributions. This phase difference ensures that interference between the two is minimal; thus the CP-odd couplings contribute predominantly to first order quadratically, whereas the contributions of the non-standard CP-even couplings can interfere with the Standard Model amplitude. The $\tilde{\lambda}_V$ terms also contribute to first order dominantly quadratically; they however have a much better high energy behaviour. They rise with energy like s, and not $\sqrt{s}$, as do the $\tilde{\kappa}$ terms. The limits on $\tilde{\lambda}_V$, as listed in Table III, are consequently much tighter than those for $\tilde{\kappa}_V$, Table II. Indeed, some of the limits on $\tilde{\lambda}_V$ from the different channels are of the same scale as predicted for these couplings by the various "beyond-Standard" models [25,26], specifically, those from the $\mu^+\tau^-$ process at 1 TeV. Also, they approach the level of precision predicted necessary by neutron electric dipole moment measurements. Of course, these limits for $\tilde{\lambda}_V$ are dependent on the choice of the scaling parameter for the $\tilde{\lambda}_V$ term in Eq. 1 (we chose m_W^2). A choice of $\Lambda = 1$ TeV, reflecting the scale of possible "new" physics, sometimes suggested as being more appropriate, would weaken the bounds on $\tilde{\lambda}_V$ by 2 orders of magnitude.

2. Improved Limits from χ^2 and Maximum Likelihood Analyses

The sensitivity to the CP-odd couplings shows the same phase space localization as was demonstrated for the CP-even couplings, with the regions of least sensitivity contributing a large portion of the total cross-section. We can account for both the high and low sensitivity

regions, and do so in a manner which optimizes both statistics and sensitivity, through a χ^2 [27] or maximum likelihood analysis [28,29]. We present briefly the basic principles of the two analyses and the scale of the limits achievable with them.

To demonstrate the principle of the χ^2 analysis, we consider a distribution where the sensitivity to $\tilde{\kappa}_V$ and $\tilde{\lambda}_V$ is small where the differential cross-section is large, and large where the differential cross-section is small (such as the angular variable θ_{τ^-}). We divide the phase space into bins, the choice of number and size of the bins roughly determined by the regions of different sensitivity. We then define our χ^2 test variable as a sum over these bins

$$\chi^2 = \sum_i^n \left[\frac{(X_i - Y_i)^2}{\Delta_i^2} \right]$$

where

$$X_i = \left(\frac{d\sigma_{NSM}}{d\cos\theta_{l^-}} \right)_i, Y_i = \left(\frac{d\sigma_{SM}}{d\cos\theta_{l^-}} \right)_i$$

and σ_{NSM} and σ_{SM} are the anomalous and standard cross-sections, respectively. Δ_i^2 combines both statistical and systematic errors for the particular bin.

$$\Delta_i^2 = (\Delta_i^{stat})^2 + (\delta^{sys} Y_i)^2$$

Where the cross-section is large, the sensitivity, and consequently the "variance" $(X_i - Y_i)^2$, is small. However, if Y_i is large, then the statistics should be improved, and Δ_i^2 will also be small. Conversely, for regions where the sensitivity is large; so also will Δ_i^2 be, due to the poorer statistics. By summing over these different regions, χ^2 gives a more accurate estimate of the deviation of the non-standard cross-section from the standard.

χ^2 was calculated from the θ_{l^-} distribution as a sum over the following three bins, $(-.95 \to -.5), (-.5 \to 0)$ and $(0 \to .95)$. With 2 degrees of freedom, the 95% C.L. corresponds to a χ^2 of 6.0. The systematic error was taken as 5%.

We determined that the limits from such a χ^2 analysis are generally improved by approximately 10%, compared to those obtained from an analysis of the total cross-section.

Even greater improvements are possible through a maximum likelihood analysis. As an example, consider the $\tilde{\kappa}_V$ dependence of the $\mu\tau$ process. We consider the two dimensional differential cross-section

$$\frac{d^2\sigma}{d(\cos\theta_{\tau^-})d(M_{\mu\tau})}$$

where θ_{τ^-} and $M_{\mu\tau}$ are as defined previously. We divide this distribution into bins and define the measured and expected number of events in a given bin as r_i and $\mu_i(\tilde{\kappa})$ respectively. If we assume that the number of events in each bin follows a Poisson distribution with a mean of μ_i, then the probability of measuring r_i events is given by

$$y_i(\mu_i(\tilde{\kappa}), r_i) = e^{-\mu_i(\tilde{\kappa})}\frac{\mu_i(\tilde{\kappa})^{r_i}}{r_i!}$$

and we define a likelihood function over all the bins as

$$L(\tilde{\kappa}) = \ln\left(\prod_i e^{-\mu_i(\tilde{\kappa})}\frac{\mu_i(\tilde{\kappa})^{r_i}}{r_i!}\right)$$

and our measure of deviation from the SM as

$$\Delta L = L(\tilde{\kappa}) - L(\tilde{\kappa}_{SM})$$

$$\Delta L = \sum_i \left[-(r_i - \mu_i(\tilde{\kappa}_{SM})) + r_i(\ln r_i - \ln \mu_i(\tilde{\kappa}_{SM}))\right]$$

where $L(\tilde{\kappa}_{SM})$ is the likelihood function $L(\tilde{\kappa})$ with the couplings taking their SM values.

We divide the $\cos\theta_{\tau^-}$ and $M_{\mu\tau}$ distributions into 5 bins each. We show in Fig. 3 the $\Delta L = 2$ contour (corresponding to a 2σ significance level) in $\tilde{\kappa}_\gamma$ and $\tilde{\kappa}_Z$ for the $\mu^+\tau^-$ process at $\sqrt{s}$ of 500 GeV. We extract limits from this contour of

$$-0.10 < \tilde{\kappa}_\gamma < 0.10$$

$$-0.11 < \tilde{\kappa}_Z < 0.12$$

which are a significant improvement on the constraints achievable from a simple total cross-section measurement. Similarly, the limits for the other parameters and other processes were generally improved by approximately 50% relative to the total cross-section limits through such an analysis.

B. CP Asymmetries as Indicators of CP Violation

A more intuitive means of identifying a CP-violating contribution is, rather than looking for non-standard effects in cross-sections, to search directly for evidence of the breaking of the symmetry. Even a small amount of CP violation in the triple boson vertex could in principle produce clear experimental signatures. These signatures could consist of asymmetries, for instance, in the numbers of events between two CP-conjugate states. As an example, in the process $e^+e^- \to W^+W^-$, a difference between the numbers of W^+ bosons emitted in the "forward" direction, and the number of W^- bosons in the "backward" direction, as it distinguishes between these CP-conjugate states, would indicate the breaking of CP. Different types of observable asymmetries have been suggested as possible indicators of CP-violation [30]; these include width asymmetries, partial rate asymmetries such as energy and angular asymmetries, and CP-odd correlations.

We search for non-zero asymmetries in certain measurable observables as evidence for a CP-violating contribution to the TBV. The observables we consider are defined in terms of the final state charged lepton and anti-lepton momenta and/or polar and azimuthal angles, and thus avoid any ambiguity from neutrino non-detection.

We define the polar and azimuthal angles of the final state lepton and anti-lepton (θ, ϕ) and $(\overline{\theta}, \overline{\phi})$ through the momentum parametrization

$$\vec{p} = |\vec{p}|(\sin\phi\sin\theta, \sin\phi\cos\theta, \cos\phi)$$
$$\vec{q} = |\vec{q}|(\sin\overline{\phi}\sin\overline{\theta}, \sin\overline{\phi}\cos\overline{\theta}, \cos\overline{\phi})$$

where $\vec{p}$ and $\vec{q}$ are the three-momenta of the outgoing charged lepton and charged antilepton, respectively. The CP operation results in the following transformation amongst the angular variables:

$$(\theta, \phi, \overline{\theta}, \overline{\phi}) \overset{CP}{\leftrightarrow} (\pi + \overline{\theta}, \pi - \overline{\phi}, \pi + \theta, \pi - \phi) \tag{6}$$

If the transition matrix M is hermitian, then $CP\tilde{T}$ invariance gives the following relation:

$$M_{\sigma\overline{\sigma};\lambda\overline{\lambda}} = M^*_{-\overline{\sigma},-\sigma;-\overline{\lambda},-\lambda}$$

The combined $CP\tilde{T}$ is therefore equivalent to the following transformation amongst the angular variables

$$(\theta, \phi, \overline{\theta}, \overline{\phi}) \overset{CP\tilde{T}}{\leftrightarrow} (\pi - \overline{\theta}, \pi - \overline{\phi}, \pi - \theta, \pi - \phi) \tag{7}$$

We can now classify angular distributions according to their behaviour under CP and $CP\tilde{T}$. In light of the previous discussion, we concentrate on CP-odd and $CP\tilde{T}$-even variables and restrict ourselves to the real parts of $\tilde{\kappa}_V$ and $\tilde{\lambda}_V$.

We examined asymmetries in the following variable, defined here as S [13]

$$S = \sin\phi \sin\theta + \sin\overline{\phi} \sin\overline{\theta}$$

If CP is a valid symmetry, then a differential cross-section in S would necessarily be symmetric about S=0. The presence of CP violating couplings such as $\tilde{\kappa}_V, \tilde{\lambda}_V$ will manifest itself in the loss of this symmetry. We define an asymmetry as

$$A^S_{CP} = \frac{\int d\sigma(S > 0) - \int d\sigma(S < 0)}{\int d\sigma(S > 0) + \int d\sigma(S < 0)} \tag{8}$$

We can also determine the asymmetries in the individual helicity amplitudes, defined analogously to that in the total cross-section. Non-zero values for these helicity asymmetries combine to produce a non-zero value for the total cross-section; it is therefore possible for large oppositely signed asymmetries in the helicities to combine to give a smaller net asymmetry in the total cross-section.

For $\tilde{\kappa}_V$ and $\tilde{\lambda}_V$ equal to 1, we show in Table IV the asymmetries A^S_{CP} in the total cross-section for the lepton channels $\mu^+\tau^-, \mu^+\mu^-$, and e^+e^-. (Although $\mu^+\tau^-$ is not a CP eigenstate, having neglected lepton masses, this channel effectively approximates the CP invariant W^+W^- production. The μ^+e^- channel, without its charge conjugate process μ^-e^+, is not CP invariant; it also introduces TBV dependent diagrams additional to those of W^+W^-). The CP-odd couplings contribute predominantly to first-order quadratically; we therefore restrict our study to positive anomalous couplings $\tilde{\kappa}_V, \quad \tilde{\lambda}_V = 1.0$.

We notice that the asymmetries are of the same magnitude for each of the different final state configurations, and that the higher energy does not guarantee larger asymmetries. The typical magnitude of these values of $\sim 10^{-3}$ agrees with the prediction of Mani *et al.* [31]. These authors, instead of simple asymmetries, looked at expectation values of CP-odd variables, and find A$\sim 10^{-3}$ for $\tilde{\kappa} = \tilde{\lambda} = 0.1$. We also considered asymmetries in the CP-odd, $CP\tilde{T}$-even variable $\vec{k}_2 \cdot (\vec{p}_1 \times \vec{q}_1)$ [24] where $\vec{k}_2$ is the vector momentum of the incoming electron, $\vec{p}_1$ that of the outgoing lepton, and $\vec{q}_1$ that of the outgoing antilepton. The results were similar to those for the variable S.

For an asymmetry in the total cross-section to be measurable, we require that the number of asymmetrical events ΔN exceed the fluctuations about the total number of events. Thus our significance requirement for these asymmetries is:

$$\Delta N > \delta N$$
$$A\sigma L > \sqrt{\sigma L}$$
$$A > (\sigma L)^{-\frac{1}{2}}$$

If we take a typical value for the cross-section of $\sigma \sim 0.1$ pb , and with our assumed integrated luminosity of 50 fb^{-1}, this significance level is approximately 1.5 %. From this quick calculation, it seems that an asymmetry in the total cross-section will most likely be below the statistical significance level, and therefore unresolvable. The situation is even less encouraging if, instead of $\tilde{\kappa}_V = \tilde{\lambda}_V = 1.0$, we explore the expected asymmetries for more realistic magnitudes for the anomalous couplings, ie. $\tilde{\kappa}_V$ and $\tilde{\lambda}_V$ at their detection limits.

Although it appears that any asymmetry in total cross-section will be below the level of statistical significance, asymmetries in the helicity amplitudes that contribute to the total cross-section might be detectable. An asymmetry in the total cross-section is a result of a combination of asymmetries in the contributing helicity amplitudes, each weighted by their appropriate helicity cross-sections. Since the different helicity amplitudes have contributions from different TBV diagrams, with consequently different sensitivity to anomalous couplings, the asymmetries in these helicity amplitudes can differ in magnitude and sign. In principle

therefore, large but opposing asymmetries can cancel each other to produce a smaller resultant asymmetry in the total cross-section. We demonstrate this idea by considering the "differential asymmetries". We define this differential asymmetry $\chi(S)$ as

$$\chi(S) = \frac{\left(\frac{d\sigma}{d(S)} - \frac{d\sigma}{d(-S)}\right)}{\sigma} \tag{9}$$

and consider both total and helicity distributions. We show in Fig. 4 the distributions in χ(S) for the $\mu^+\tau^-$ channel at $\sqrt{s} = 500$ GeV for non-standard $\tilde{\kappa}_Z = 1.0$. As was previously mentioned, we use the $\mu^+\tau^-$ channel to approximate the W^+W^- process. We show also the approximate statistical error bars about the SM expectation of χ(S)=0, calculated from the differential cross-section $d\sigma/dS$. For SM couplings, $\chi(S)$ vanishes for each helicity individually.

We see that while the asymmetry in the total cross-section, as it is bounded by the error bars, would be below the statistical significance level and so unresolvable; that in the $(+-+-)$ helicity amplitude might however be measurable. A polarized beam facility, by separately generating the different helicity components, might be able to measure these helicity asymmetries and so access this phenomena.

IV. CONCLUSIONS

We have presented an analysis of the sensitivity to the WWV coupling parameters through measurement of the processes $e^+e^- \to l^+\nu l^{-\prime}\overline{\nu}$ at center-of-mass energies of 500 GeV and 1 TeV. The limits on the CP-even coupling κ_V are of the order of 1% at the higher energy, with slightly looser bounds achievable at the lower energy. These bounds might be significantly improved at a polarized beam facility. Because the individual helicity amplitudes can have very different dependence on the TBV, in form and magnitude, the limits obtainable from an analysis of an individual helicity amplitude can be complementary to those from the other helicities and from a total cross-section analysis. Consequently, combining the limits from the different helicity amplitudes can, for certain of the four lepton

final state configurations, significantly tighten the constraints on the anomalous couplings. Smaller improvements are also possible through suitably cutting on the phase space of certain experimental variables. The sensitivity to anomalous couplings is not always evenly distributed over these variable's distributions; a cut to isolate the regions of high sensitivity and exclude those of low sensitivity can improve the achievable TBV bounds. These improvements can be of the order of a factor of two for the $\mu^+\tau^-$ process at the lower energy.

The limits on the CP-odd coupling $\tilde{\lambda}_V$, especially at the higher energy, approach the level of precision predicted necessary by neutron electric dipole moment measurements; the limits on the CP-odd variable $\tilde{\kappa}_V$ are much looser. These limits can be improved by accounting for the uneven localization of TBV sensitivity in certain experimental variables through a χ^2 analysis or a maximum likelihood fit.

An explicitly CP-violating vertex contribution is unlikely to produce measurable asymmetries in the total cross-section. Asymmetries in certain CP-odd variables might however be measurable in the component helicity amplitudes; a polarized beam facility would be required for this measurement.

ACKNOWLEDGEMENTS

This work was funded in part by the Natural Sciences and Engineering Council of Canada. The authors thank Mikulas Gintner and W.Y. Keung for helpful discussions.

REFERENCES

[1] M. Davier et al., in *Proceedings of the ECFA Workshop on LEP 200*, Aachen, Germany, 1986, edited by A. Bohm and W. Hoogland, (CERN Report No. 87-08, Geneva, Switzerland, 1987) 120.

[2] G.L. Kane, J. Vidal, and C.P. Yuan, *Phys. Rev.* **D39** (1989) 2617.

[3] *Proceedings of the Workshop on Physics and Experiments with Linear e^+e^- Colliders*, Waikoloa, Hawaii, 1993, edited by F. Harris *et al.*, (World Scientific, 1994).

[4] *Proceedings of the Workshop on e^+e^- Collisions at 500 GeV: the Physics Potential*, edited by P. Zerwas, (DESY Report No. 92-123B, Hamburg, Germany, 1992).

[5] *Proceedings of the Workshop on Physics and Experiments with Linear Colliders*, Saariselkä, Finland, 1991 (World Scientific, 1992), edited by P. Eerola *et al.*

[6] F. Abe *et al.*, (CDF Collaboration), *Phys. Rev. Lett.* **74**, 1936 (1995).

[7] J. Ellison, (D0 Collaboration), FERMILAB-Conf-94/329-E (November 1994), to appear in the Proceedings of the *Eighth Annual Meeting of the American Physical Society, Division of Particles and Fields*, Alburquerque, NM (1994).

[8] T.A. Fuess, (CDF Collaboration), FERMILAB-Conf-94/283-E, (September 1994), to appear in the Proceedings of the *Eighth Annual Meeting of the American Physical Society, Division of Particles and Fields*, Alburquerque, NM (1994); F. Abe *et al.*, (CDF Collaboration), FERMILAB-Conf-94/158-E (June 1994), contributed paper to the *27th International Conference on High Energy Physics*, Glasgow, Scotland, July 1994; F. Abe *et al.*, (CDF Collaboration), FERMILAB-Pub-95/036-E (March 1995), submitted to *Phys. Rev. Lett.*

[9] S. Abachi *et al.* (D0 Collaboration), FERMILAB-Pub-95/044- E, (March 1995), submitted to *Phys. Rev. Lett.*

[10] R. Ammar *et al.*, (CLEO Collaboration), *Phys. Rev. Lett.*, **71**, 674 (1993).

[11] X-G. He and B. McKellar, *Phys. Lett.*, **B320**, 165 (1994).

[12] R. Martinez, M.A. Perez, and J.J. Toscano, *Phys. Lett.*, **B340**, 91 (1994).

[13] K. Hagiwara, R.D. Peccei, D. Zeppenfeld, and K. Hikasa, *Nucl. Phys.* **B282**, 253 (1987).

[14] G. Couture, S. Godfrey, and R. Lewis, *Phys. Rev.* D **45**, 777 (1992).

[15] P. Kalyniak *et al.*, *Phys. Rev.* D **48**, 5081 (1993); Doctoral Thesis, Paul Madsen, Carleton University, 1994.

[16] H. Aihara *et al.*, *Summary of the DPF Working Subgroup on Anomalous Gauge Boson Interactions of the DPF Long Range Planning Study*, FERMILAB-Pub-95-01, MAD/PH/871, UB-HET-95-01, UdeM-GPP-TH-95-14, March 1995.

[17] G. Couture *et al.*, *Phys. Rev.* D **36**, 859 (1987).

[18] G. Couture *et al.*, *Phys. Rev.* D **38**, 860 (1988).

[19] M.B. Einhorn, in *Proceedings of the Workshop on Physics and Experiments with Linear e^+e^- Colliders*, Waikoloa, Hawaii, 1993, edited by F. Harris *et al.*, (World Scientific, 1994) 122.

[20] W. Marciano and A. Queijiero, *Phys. Rev.* D **33**, 3449 (1986); F. Boudjema *et al.*, *ibid* **43**, 2223, (1991).

[21] D.H. Perkins, in *Proceedings of the ECFA Workshop on LEP 200*, Aachen, Germany, 1986, edited by A.Bohm and W.Hoogland, (CERN Report No. 87-08, Geneva, Switzerland, 1987) 1.

[22] C.L. Bilchak and J.D Stroughair, *Phys. Rev.* D**30** , 1881 (1984).

[23] A.A. Likhoded *et al.*, IC/93/288, October 1993.

[24] D. Chang *et al.*, *Phys. Rev.* **D48**, 4045 (1993).

[25] X.G. He *et al.*, *Phys. Lett.* **B**304 (1993) 285.

[26] D. Chang *et al.*, *Nucl. Phys.* **B355**, 295 (1991)

[27] S.Y. Choi and F. Schrempf, *Phys. Lett.* **B**272 (1991) 149.

[28] T.L. Barklow, SLAC-PUB-5808, April 1992.

[29] M. Gintner, private communication

[30] S.D. Rindani, *CP Violation at Colliders*, talk given at WHEPP3, Madras, India, 1993.

[31] H.S. Mani, B. Mukhopadhyaya, and S. Raychaudhari, M.R.I, Allahabad preprint, MRI-PHY/9/93(1993).

FIGURES

FIG. 1. $\pm 2\sigma$ contour plots for $(+-+-)$ helicity amplitude (solid line) and $(-++-)$ helicity amplitude (dashed line) of $\mu^+\tau^-$ channel at $\sqrt{s} = 500$ GeV.

FIG. 2. Differential cross-sections with respect to (a) $\cos\theta_{\tau^-}$ for Standard Model(solid line), $\Delta\kappa_\gamma = \Delta\kappa_Z = -0.1$(dashed line), and $\Delta\kappa_\gamma = \Delta\kappa_Z = 0.1$(dotted line).

FIG. 3. $\Delta L = 2$ contour in $\tilde{\kappa}_\gamma$ and $\tilde{\kappa}_Z$ for maximum likelihood analysis for $\mu^+\tau^-$ process at $\sqrt{s} = 500$ GeV.

FIG. 4. Distributions in χ(S) for the $\mu^+\tau^-$ process at center-of-mass energy of 500 GeV with $\tilde{\kappa}_Z = 1.0$. The solid line corresponds to the total cross-section, the dot-dashed to the $(-++-)$ amplitude, and the dashed to the $(+-+-)$ amplitude. The asymmetries are divided by the appropriate cross-section, either total or component. The dotted line represents the statistical error bounds.

TABLES

TABLE I. 2σ limits for various cut combinations for $\mu^+\tau^-$ process at $\sqrt{s} = 500$ GeV.

Cuts	$\Delta\kappa < 0$	$\Delta\kappa > 0$
$\theta_C = 0.95$	1.5%	9.3%
$\theta_C = 0.9$	1.2%	9.3%
$\theta_C = 0.7$	0.8%	9.0%
$\theta_C = 0.7, 30 < M_{\mu\tau} < 430$	1.0%	8.5%
$\theta_C = 0.7, 100 < M_{\mu\tau} < 350$	0.79%	9.0%

TABLE II. 2σ bounds on non-standard couplings $\tilde{\kappa}_V$

Process	$\sqrt{s}$ (GeV)	Sensitivity Limits
$\mu\tau$	500	$-0.19 < \tilde{\kappa}_\gamma < 0.18 \quad -0.16 < \tilde{\kappa}_Z < 0.16$
	1000	$-0.13 < \tilde{\kappa}_\gamma < 0.13 \quad -0.12 < \tilde{\kappa}_Z < 0.12$
μe	500	$-0.17 < \tilde{\kappa}_\gamma < 0.18 \quad -0.17 < \tilde{\kappa}_Z < 0.18$
	1000	$-0.14 < \tilde{\kappa}_\gamma < 0.15 \quad -0.15 < \tilde{\kappa}_Z < 0.15$
$\mu\mu$	500	$-0.24 < \tilde{\kappa}_\gamma < 0.24 \quad -0.18 < \tilde{\kappa}_Z < 0.17$
	1000	$-0.21 < \tilde{\kappa}_\gamma < 0.21 \quad -0.10 < \tilde{\kappa}_Z < 0.10$
ee	500	$-0.17 < \tilde{\kappa}_\gamma < 0.17 \quad -0.19 < \tilde{\kappa}_Z < 0.19$
	1000	$-0.15 < \tilde{\kappa}_\gamma < 0.15 \quad -0.11 < \tilde{\kappa}_Z < 0.11$

TABLE III. 2σ bounds on non-standard couplings $\tilde{\lambda}_V$

Process	$\sqrt{s}$ (GeV)	Sensitivity Limits
$\mu\tau$	500	$-0.013 < \tilde{\lambda}_\gamma < 0.012 \quad -0.011 < \tilde{\lambda}_Z < 0.011$
	1000	$-0.00098 < \tilde{\lambda}_\gamma < 0.00095 \quad -0.00090 < \tilde{\lambda}_Z < 0.00087$
μe	500	$-0.0073 < \tilde{\lambda}_\gamma < 0.00074 \quad -0.0070 < \tilde{\lambda}_Z < 0.0068$
	1000	$-0.00077 < \tilde{\lambda}_\gamma < 0.00079 \quad -0.00084 < \tilde{\lambda}_Z < 0.00081$
$\mu\mu$	500	$-0.015 < \tilde{\lambda}_\gamma < 0.015 \quad -0.014 < \tilde{\lambda}_Z < 0.014$
	1000	$-0.0016 < \tilde{\lambda}_\gamma < 0.0016 \quad -0.0014 < \tilde{\lambda}_Z < 0.0014$
ee	500	$-0.011 < \tilde{\lambda}_\gamma < 0.011 \quad -0.010 < \tilde{\lambda}_Z < 0.0095$
	1000	$-0.0013 < \tilde{\lambda}_\gamma < 0.0013 \quad -0.0013 < \tilde{\lambda}_Z < 0.0012$

TABLE IV. Asymmetries $A_{CP}^S(\times 10^3)$ in Total Cross-Section

Process	$\sqrt{s}$ (GeV)	$\tilde{\kappa}_\gamma = 1$	$\tilde{\kappa}_Z = 1$	$\tilde{\lambda}_\gamma = 1$	$\tilde{\lambda}_Z = 1$
$\mu\tau$	500	-2.1	-3.3	-1.9	-1.8
	1000	0.58	1.1	-1.9	-2.0
$\mu\mu$	500	-1.3	-0.67	3.2	3.9
	1000	-0.14	-1.7	-1.1	-1.3
ee	500	-2.2	-2.5	-3.7	-4.1
	1000	0.16	0.85	-6.3	-6.7

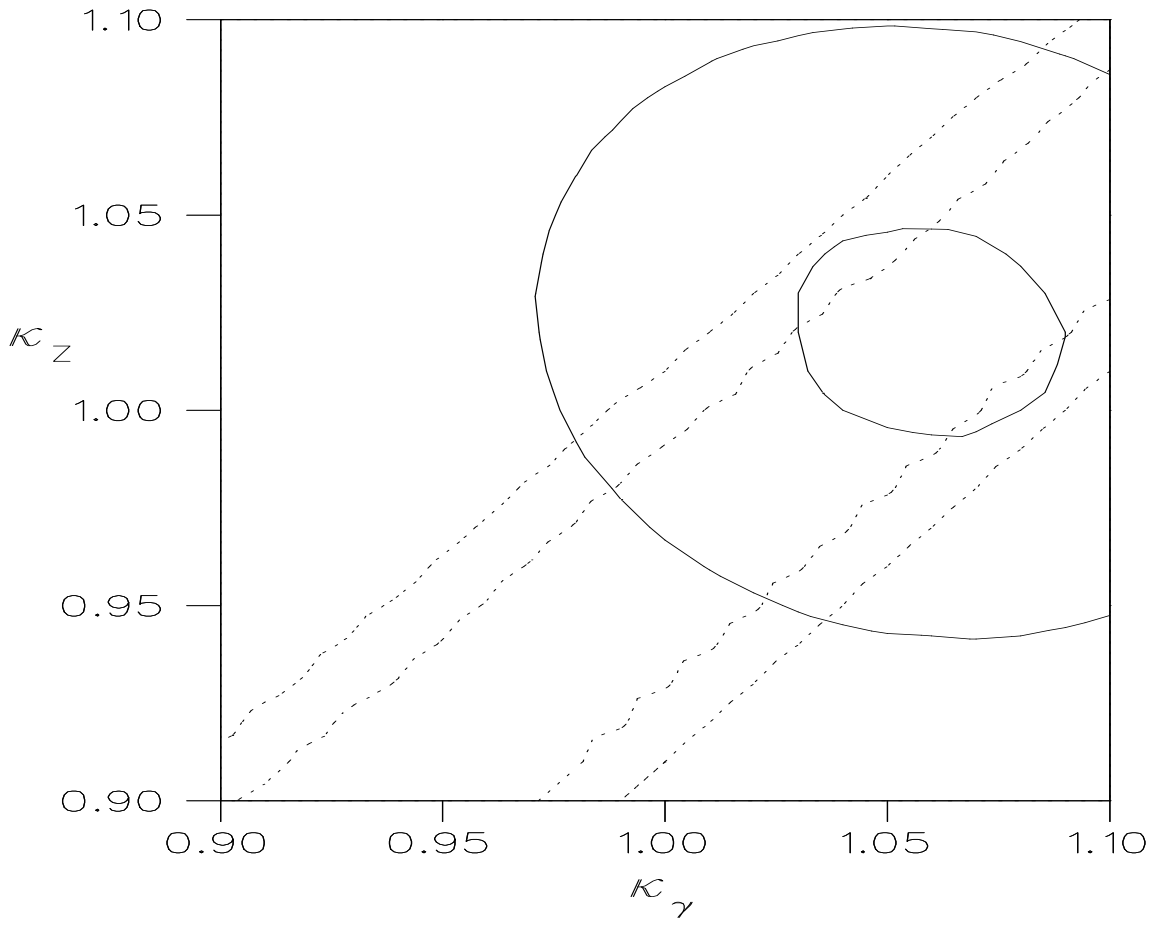

Fig. 1

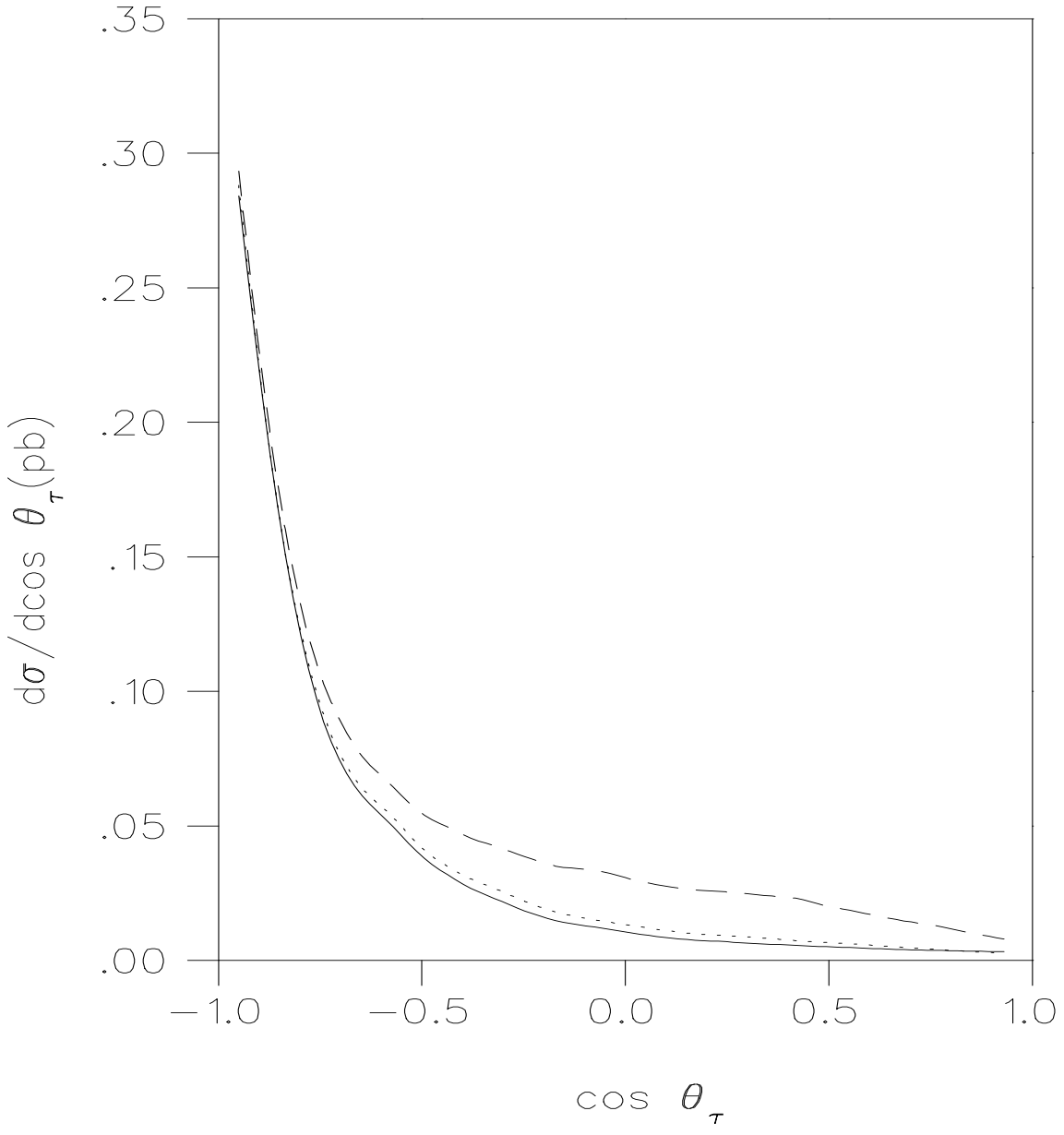

Fig. 2

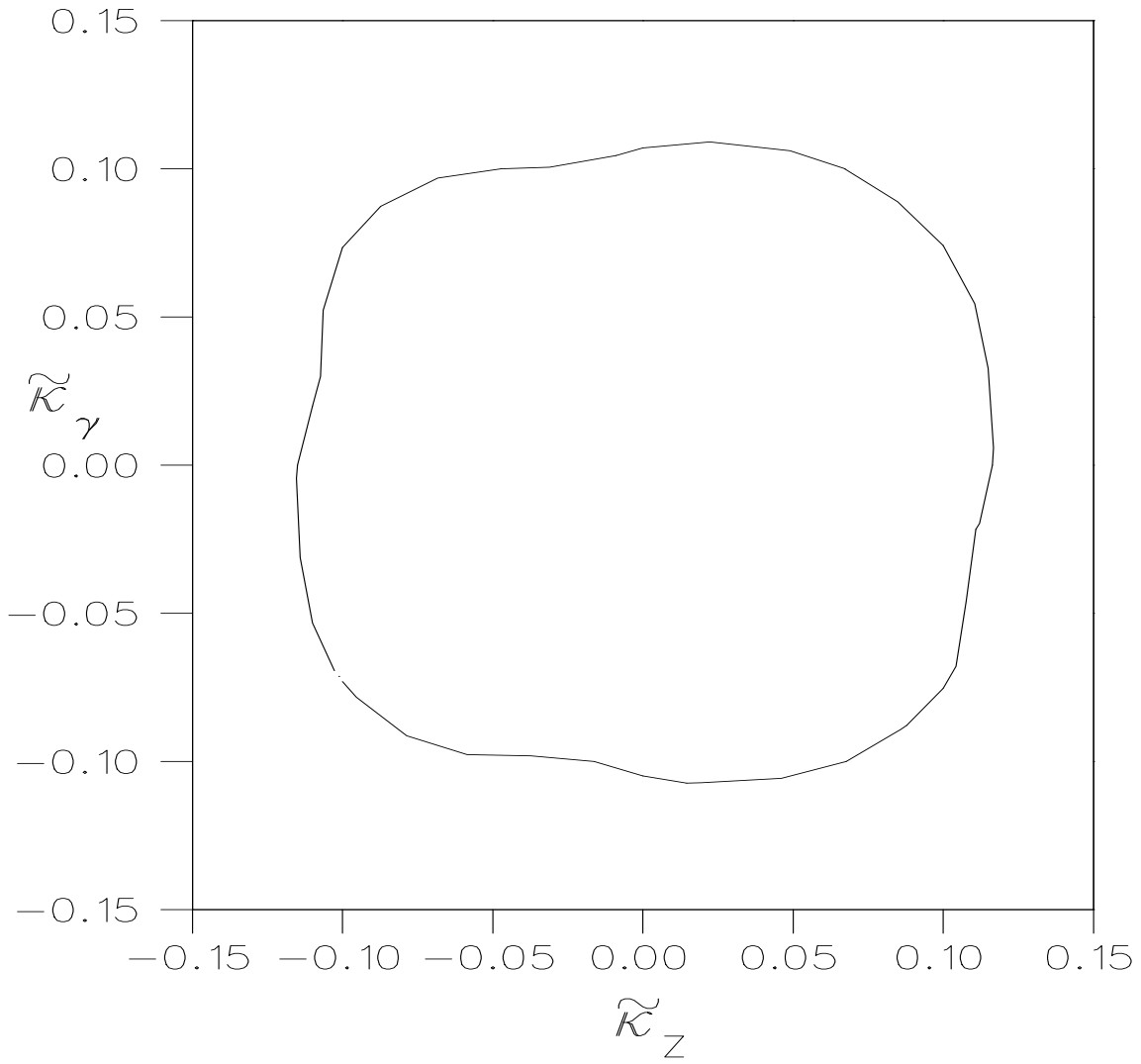
0.15
0.10
0.05
$\widetilde{\kappa}_\gamma$
0.00
−0.05
−0.10
−0.15
−0.15 −0.10 −0.05 0.00 0.05 0.10 0.15
$\widetilde{\kappa}_Z$

Fig. 3

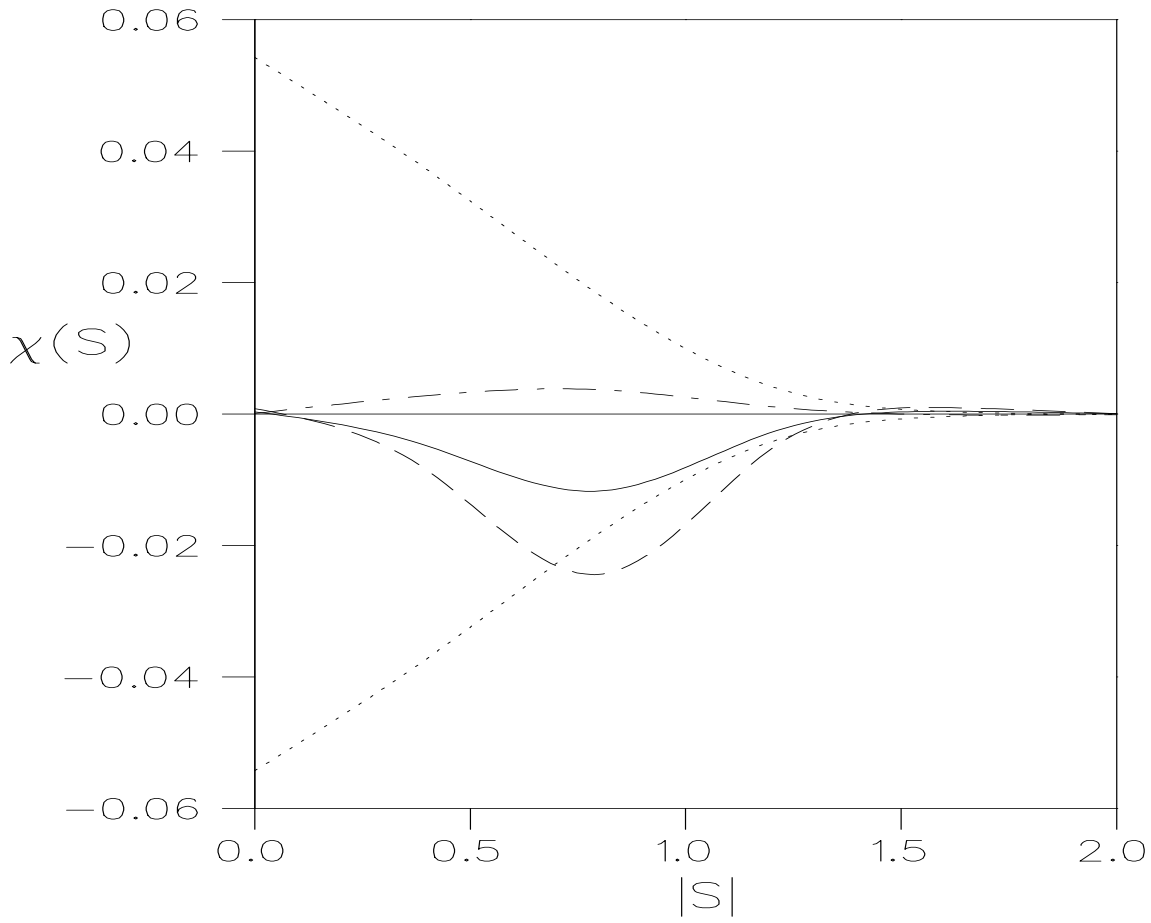

Fig. 4